

**Removal of fluoride ions from aqueous solutions and water for human consumption by a surfactant modified zeolite****Eliminación de iones fluoruro de soluciones acuosas y agua para consumo humano mediante una zeolita modificada con un tensioactivo**N. Flores-Alamo¹, J.I. Vázquez-Méndez^{1,2}, M.J. Solache-Ríos², F. Cuellar-Robles¹, M.C. Carreño-de-León^{1*}¹*División de Estudios de Posgrado e Investigación, Tecnológico Nacional de México/Instituto Tecnológico de Toluca, Av. Tecnológico s/n. Colonia Agrícola Bellavista, Metepec, Estado de México, C.P. 52149, México.*²*Departamento de Química, Instituto Nacional de Investigaciones Nucleares, Carretera México-Toluca S/N, La Marquesa, Ocoyoacac, Estado de México C.P. 52750, México.*

Received: December 27, 2024; Accepted: March 13, 2025

Abstract

Fluoride ions are found in groundwater due to the presence of some minerals like fluorite (CaF_2) and fluorapatite ($\text{Ca}_5(\text{PO}_4)_3\text{F}$). A clinoptilolite type zeolite was modified with hexadecyltrimethylammonium bromide in order to determine its adsorption properties for the removal of fluoride ions from water, the material was characterized by Fourier transform infrared spectroscopy, scanning electron microscopy, X-ray diffraction and the point of zero charge was determined. Sorption experiments were performed by using a solution of sodium fluoride and water from the state of Zacatecas, México. The kinetic data were adequately fitted to the pseudo first-order model, and the isotherms data to the Freundlich model, suggesting that the sorption process is carried out by physisorption on a heterogeneous material, the adsorption was similar between 20 and 50°C and the highest adsorption was between pH 4 and 6. Experiments carried out with water from the state of Zacatecas showed a removal of 86.3 % with 130 mg of modified zeolite and 10 mL of water. The results show that this material is an alternative for removing fluoride ions from water.

Keywords: fluoride ions, adsorption, zeolite, pollution.

Resumen

Los iones de fluoruro se encuentran en el agua subterránea debido a la presencia de algunos minerales como la fluorita (CaF_2) y la fluorapatita ($\text{Ca}_5(\text{PO}_4)_3\text{F}$). Se modificó una zeolita tipo clinoptilolita con bromuro de hexadeciltrimetilamonio con el fin de determinar su capacidad de adsorción para la remoción de iones fluoruro del agua, el material se caracterizó mediante espectroscopia de infrarrojo por transformada de Fourier, microscopía electrónica de barrido, difracción de rayos X y se determinó el punto de carga cero. Los experimentos de sorción se realizaron utilizando una solución de fluoruro de sodio y agua del estado de Zacatecas, México. Los datos cinéticos se ajustaron adecuadamente al modelo de pseudo primer orden, y los datos de isoterma al modelo de Freundlich, sugiriendo que el proceso de sorción se realiza por fisisorción sobre un material heterogéneo, la adsorción fue similar entre 20 y 50°C y la capacidad máxima de adsorción estuvo entre un pH de 4 y 6. Los experimentos realizados con agua del estado de Zacatecas mostraron una remoción del 86.3 % con 130 mg de zeolita modificada y 10 mililitros de agua. Los resultados muestran que este material es una alternativa para la eliminación de iones fluoruro del agua.

Palabras clave: iones fluoruro, adsorción, zeolita, contaminación.

* Corresponding author. E-mail: mcarrenod@toluca.tecnm.mx ;

<https://doi.org/10.24275/rmiq/IA25491>

ISSN:1665-2738, issn-e: 2395-8472

1 Introduction

Clean and accessible water for human consumption is one of the greatest challenges (Alarcón-Herrera *et al.* 2020). Due to the increase of population, water demand for irrigation, industrial and domestic uses has increased considerably and turned groundwater into an important source (Chai *et al.* 2022; Serrano-Mesa *et al.* 2024), almost 50 % of the population uses groundwater, however, its quality may be compromised due to the presence of some chemical species like fluoride ions (López-Guzmán *et al.* 2019). An example of this is Zacatecas, a state located in the central north area of the Mexican territory with a dry, semi-dry climate temperate and semi-humid zone (Martínez-Salazar *et al.* 2016). In this region, there are numerous mineral deposits linked to the western Sierra Madre, which are mainly composed of feldspars, limestone, quartz, calcite, cryolite and some clays (Alarcón-Herrera *et al.* 2020).

Fluoride ions are commonly found in minerals that are in contact with groundwater (He *et al.* 2020), their concentrations are generally associated with the geographical regions and the degree of water-minerals interactions (Navarro *et al.* 2017). Fluoride ions are classified among the twelve most dangerous pollutants by the Agency for Toxic Substances and the United States Disease Registry (ATSDR) due to their great reactivity and toxicity (Nizam *et al.* 2022).

Fluoride ions have severe effects on bones and teeth because they displace hydroxide ions from hydroxyapatite, the main mineral component of teeth and bones, to form fluorapatite. Fluorapatite makes teeth and bones more brittle at a high concentration of fluoride ions, a condition known as dental and skeletal fluorosis (Mohapatra *et al.* 2009). Furthermore, fluoride ions may accumulate in soft tissues causing toxic effects in kidneys, heart, reproductive system and brain (Jiang *et al.* 2019).

Currently, more than 25 countries have reported that their water sources have concentrations of fluoride ions above the maximum permissible limit, set at 1.5 mg/L by the World Health Organization (WHO) and more than 300 million people suffer from different types of fluorosis (Alhassan *et al.* 2020).

Multiple technologies have been developed for the removal of fluoride ions, like adsorption, coagulation, precipitation, ion exchange, reverse osmosis, and electrodialysis (Bhatnagar *et al.* 2011). Adsorption has proven to be a simple technology, the nature of the adsorbents is the key for its efficiency, and multiple studies have been carried out to develop high-efficient adsorbents from various materials (Chen *et al.* 2022; Leal-Perez *et al.* 2024).

Zeolites are crystalline aluminosilicates that can be used as adsorbents, they have high

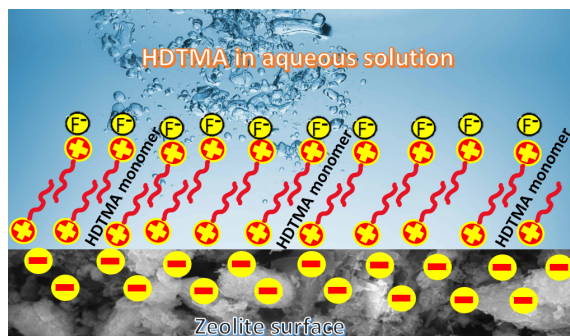


Figure 1 Schematic diagram of zeolite modification by HDTMA and fluoride interaction.

cation exchange capacities and high sorption capacities for different types of chemical species, their cation exchange capacities are due to their content of exchangeable cations such as sodium, calcium, potassium and magnesium (Znak *et al.* 2021).

One of the most abundant zeolites is clinoptilolite, which belongs to the heulandite family and has a Si/Al ratio > 4 (Saucedo-Delgado *et al.* 2017). Zeolites have been modified with organic compounds such as hexadecyltrimethylammonium bromide (HDTMA-Br) to remove anions and organic matter from water (Bajda and Kłapyta, 2013). The treatment of zeolite with HDTMA-Br (Figure 1) allows to change the surface charge of the zeolite from negative to positive, the surfactant molecules occupy the cationic exchange sites of the zeolite and form an organic coating, and the positive charge of the surface allows the removal of anions such as fluoride (Barczyk *et al.* 2014).

The objective of this work was to modify and characterize a natural zeolitic material with a surfactant and to determine its behavior in removing fluoride ions from aqueous solutions and drinking water, in order to find a new alternative for the removal of fluoride ions from drinking water.

2 Materials and methods

A natural zeolitic material obtained from Valey of Etlá municipality, located about 17 kilometers north of Oaxaca City, Mexico ($17^{\circ}12'22.14''$ N $-96^{\circ}47'56.04''$ W) was used, it was ground and sieved to 30 mesh to obtain a particle size of 0.6 mm (Corral-Capulin *et al.* 2018), Jalmek brand analytical grade reagents: hexadecyltrimethylammonium bromide (HDTMA), sodium chloride, sodium fluoride, and silver nitrate, as well as distilled water were used for the preparation of solutions.

2.1 Modification of the zeolitic material

The previously ground and sieved zeolitic material was washed with distilled water and dried at room

temperature for 24 hours. Subsequently, the zeolitic material was put in contact with 500 mL of a 2 M NaCl solution at room temperature (20°C) for 96 hours, then the supernatant was drained and the material was washed with distilled water until the chloride ions were not detected in the washing solutions by the AgNO₃ test, then it was dry at room temperature and labeled as ZS. Finally, the zeolite was put in contact with a solution of 60 mmol/L of HDTMA for 120 hours at 30°C (Dávila *et al.* 2016) and it was washed with distilled water to eliminate the excess of surfactant, the zeolitic material was identified as ZM.

2.2 Characterization of the modified zeolitic material

A JEOL JSM 6610LV scanning electron microscope was used to observe the morphology of the natural zeolitic material (ZN) and the modified one (ZM), the micrographs were taken at a magnification of 10 000, 5 000 and 3 000 x, subsequently elemental microanalysis was performed by X-ray dispersive spectroscopy (EDS).

The point of zero charge was determined as follows: 10 mL distilled water was placed in beakers and the pH of the solutions was adjusted between two and eleven by adding 0.1 M of HCl or NaOH solutions, samples of 100 mg of zeolitic material were added to each solution and shaken for 24 hours, then the phases were separated and the pH was measured by using a Hanna instruments model HI 2221 potentiometer.

A Fourier transform infrared spectrophotometer was used to obtain the spectra of the zeolitic materials, the equipment worked in transmittance analysis mode in a range from 4000 to 400 cm⁻¹.

The ZS and the ZM were analyzed by X-ray diffraction using the D8 Advance Bruker diffractogram under a range of 5-75 2θ, a step of 0.03 and a voltage of 35 kV, to identify the mineral phases of the zeolitic materials, the patterns of diffraction were compared with those of the Joint Committee of Powder Diffraction Standards cards (JCPDS).

2.3 Effect of pH

Samples of 100 mg of zeolitic material (ZM) were put in contact with 10 mL aliquots of a solution with a concentration of 10 mg/L of fluoride ions and pH between 3 and 10. They were left in contact for 9 hours with constant shaking at 20° C (Dávila *et al.* 2016), then, the phases were separated and the final concentrations of fluoride ions in the liquid phase were measured, the experiments were carried out in triplicate.

2.4 Effect of temperature

Sorption isotherms were performed at 20, 30, 40 and 50°C, 100 mg of modified zeolitic material were contacted with 10 mL of solutions of fluoride ions with concentrations from 2 to 20 mg/L at a pH of 6 and 100 rpm, the experiments were performed in triplicate.

2.5 Adsorption kinetics

100 mg samples of modified zeolitic material were put in contact with 10 mL aliquots of a 10 mg/L of fluoride ions solution at pH 6. They were kept under stirring for different contact times between 0.25 and 72 hours at 20°C and 100 rpm (Naghash and Nezamzadeh-Ejhi, 2015), the samples were separated and the concentrations of fluoride ions in the liquid phases were analyzed by using a selective electrode. The experimental data were treated with the pseudo first order (Eq. 1), pseudo second order (Eq. 2) and the Elovich models (Eq. 3) using the Origin Lab software (Liu *et al.* 2021).

$$q_t = q_e (1 - e^{-k_1 t}) \quad (1)$$

where q_t (mg/g) is the amount adsorbed at time t , q_e (mg/g) is the amount adsorbed at equilibrium and k_1 (min⁻¹) is the adsorption rate constant.

$$q_t = \frac{t}{\frac{1}{k_2 q_e^2} + \frac{t}{q_e}} \quad (2)$$

where k_2 is the kinetic constant (g/mg*min) and q_e (mg/g) is the amount adsorbed at equilibrium time.

$$q_t = \frac{1}{\beta} \ln(\alpha\beta) + \frac{1}{\beta} \ln(t) \quad (3)$$

where q_t is the amount of adsorbate adsorbed at time t , α is the initial adsorption rate (mg/g min) and β is the desorption constant (g/mg).

2.6 Adsorption isotherm

100 mg samples of zeolitic material were put in contact with 10 mL aliquots of fluoride ion solutions with concentrations of fluoride ions from 2 to 20 mg/L at pH 6. The mixtures were kept under constant stirring at 20°C, then, they were separated and the aqueous phases were analyzed to determine the concentration of fluoride ions, the experimental data were treated with the Langmuir (Eq. 4) and Freundlich (Eq. 5) models (Ahamad *et al.* 2018) with the help of the software OriginLab.

$$q_e = \frac{q_m b C_e}{1 + b C_e} \quad (4)$$

where q_e is the amount of fluoride ions absorbed per unit mass (mg/g) and C_e is the equilibrium

concentration of adsorbate in the liquid phase (mg/L) at equilibrium, b (L/mg) is the adsorption equilibrium constant and q_m is the maximum adsorption capacity (mg/g).

$$q_e = K_F C_e^{\frac{1}{n}} \quad (5)$$

where q_e is the amount of fluoride ions absorbed per unit mass (mg/g), C_e is the equilibrium concentration of the adsorbate in the liquid phase (mg/L) and K_F is the Freundlich constant (mg/g) and n is the Freundlich exponent.

2.7 Adsorption of fluoride ions from drinking water

The drinking water sample was from an urban deep well from Ojo Caliente town in the state of Zacatecas, Mexico (22°34'0.00" N -102°15'0.00" W). It was transported in a 5 L polyethylene container at 4°C as indicated by the NOM-014-SSA1-1993 standard, the sample had a pH of 7.8 and an electrical conductivity of 1532 μ mhos/cm. Aliquots of 10 mL of water with adjusted pH of 6 were put in contact with samples (between 10 and 130 mg) of the modified zeolitic material (ZM) for nine hours.

3 Results and discussion

3.1 Adsorbent characterization

Figure 2 shows the micrographs obtained from the natural and the modified zeolitic material, some particles are amorphous and other show the typical morphology of the clinoptilolite zeolite: crystals of monoclinic symmetry of blades and laths and some of them have a coffin shape (Jiménez-Reyes *et al.* 2021) and the morphology of the material was not affected after the modification. The presence of internal cavities of the material is observed as a honeycomb distribution.

The elemental analysis (SEM-EDS) is shown in Table 1, the main elements found were O, Na, Al, Si and C. Oxygen, silicon and aluminum have the highest percentages, they are the main components of the tetrahedrons that make up the zeolite network. The increase of the carbon after modification indicates the presence of the surfactant on the zeolitic material (Wingenfelder *et al.* 2006). The Si/Al ratio of the ZM sample is 5.11, this value corresponds to clinoptilolite-type zeolites.

Figure 3 shows pH vs. $pH_i - pH_f$, the value of the point of zero charge determined for the modified zeolitic material was 7.06. The point where the Y axis is intercepted corresponds to the point where the surface charge is zero, the number of negative and

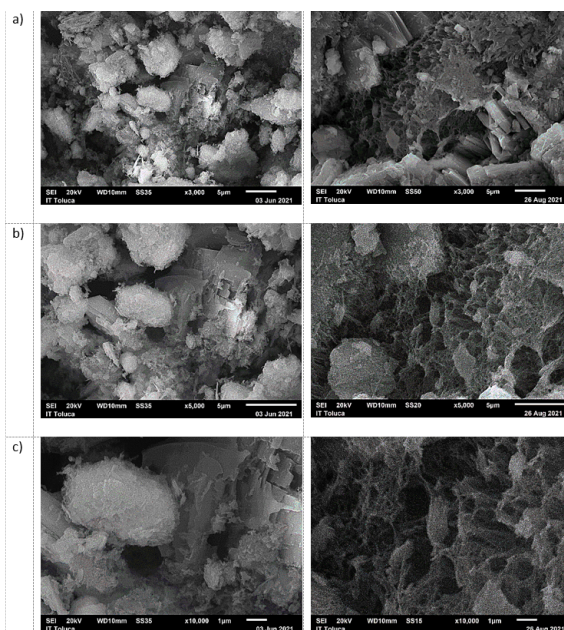


Figure 2 Micrographs of the natural zeolitic material (left) and the modified one (right) with magnifications of a) 3 000, b) 5 000 and c) 10 000 x.

Table 1 Elemental analysis of zeolitic material and modified one.

Element	% Weight	
	ZN	ZM
O	54.44 ± 1.62	50.76 ± 1.13
Na	1.70 ± 0.19	4.08 ± 0.10
Al	6.31 ± 0.57	6.28 ± 0.36
Si	33.55 ± 1.67	32.10 ± 0.65
C	4.00 ± 0.06	6.78 ± 0.31

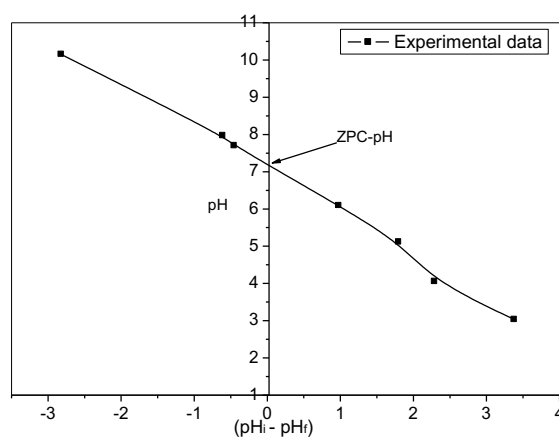


Figure 3. pH vs. $pH_i - pH_f$ for the determination of the point of zero charge of the modified zeolitic material.

positive charges are the same, the surface charge is negative at a pH higher than the point of zero charge and positive at a pH values lower than the point of zero charge (Ullah *et al.* 2020), the positive charge would attract the fluoride ions.

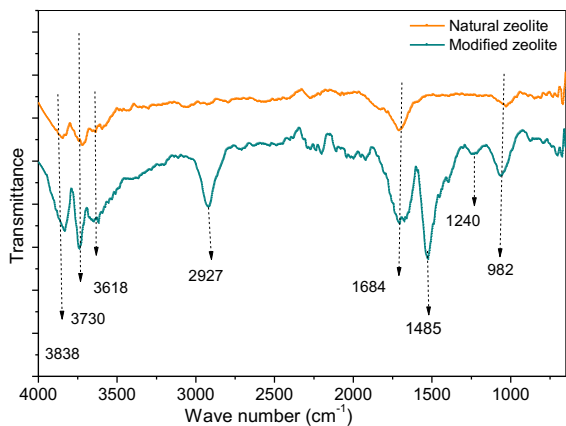


Figure 4 Fourier transform infrared spectra of the natural and modified zeolitic materials.

The Fourier transform infrared spectrum of the natural zeolitic material and the modified one presented in Figure 4, shows the bands at 3838 and 3730 cm^{-1} are related to the O-H bond stretching vibration (Hosseini *et al.* 2020). The band at 3618 cm^{-1} corresponds to the Si-OH-Al bond (Dávila *et al.* 2016), the band observed at 1684 cm^{-1} is assigned to the bending vibration of the H-O-H bond due to water (Dimas *et al.* 2021), finally, the band observed at 982 cm^{-1} corresponds to the stretching vibration of the Si-O bond present in the primary structural unit of the SiO_4 tetrahedron (Kabuba and Banza, 2020). On the other hand, a peak is observed at 1240 cm^{-1} in the spectrum of the modified zeolite related to the Al-O bond of the primary structural unit of the zeolite, the peak at 2927 corresponds to the CH_2 stretching vibrations of the aliphatic compounds in the HDTMA surfactant and the peak at 1485 cm^{-1} to the C-H stretching vibrations (Zeng *et al.* 2010), both peaks can confirm the presence of the surfactant in the zeolitic material and coincides with the results obtained by scanning electron microscopy that confirms the modification (Solińska and Bajda, 2022).

Figure 5 shows the diffractogram of the sodium zeolitic material, the main peaks correspond to the diffraction pattern of a clinoptilolite, they are located at 9.8° (0 2 0) and 11.1° (2 0 0) according to the JCPDS card 44-1398 (Saadat and Nezamzadeh- Ejjieh, 2016),

the peaks corresponding to quartz are at 20.83° (1 0 0) and 26.644° (1 0 1) according to the JCPDS file 05-0490 (Nezamzadeh-Ejjieh and Tavakoli-Ghinani, 2014), albite has characteristic peaks at 13.76° (0 2 0) and 13.92° (0 0 1) corresponding to the JCPDS card 10-0393 and finally, the characteristic peaks of heulandite are found at 7.45° (1 1 0) and 9.91° (0 2 0) (JCPDS card 75-1712).

Figure 6 shows the diffractogram of the modified zeolitic material, as can be seen, the diffractogram is like the one of the sodium zeolitic material, indicating that after the modification process, the primary structure of the material remains the same and that the modification was carried out superficially (Dimas *et al.* 2021).

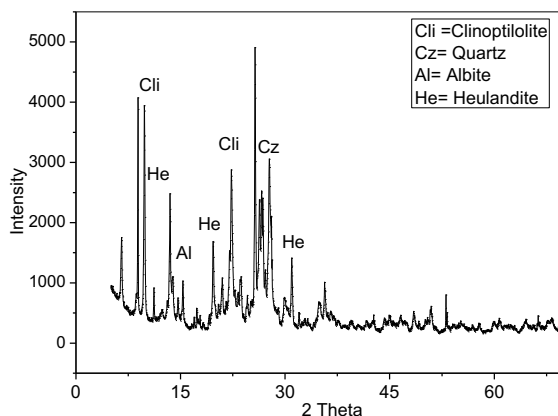


Figure 5. Diffractogram of sodium zeolitic material.

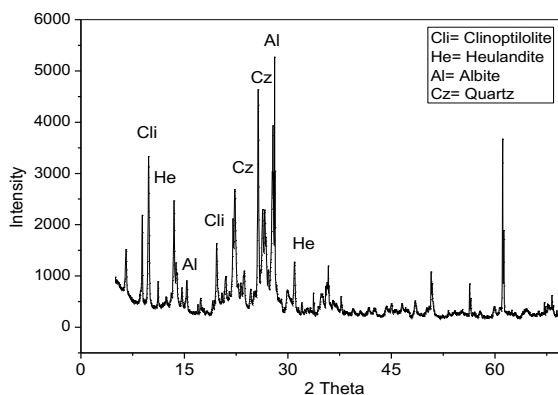


Figure 6. Diffractogram of modified zeolitic material.

Table 2. Main components of zeolitic materials.

Component	JCPDS	Chemical formula
Clinoptilolite-Ca	39-1383	$\text{KNa}_2\text{Ca}_2(\text{Si}_{29}\text{Al}_7)\text{O}_{72}\cdot 24\text{H}_2\text{O}$
Clinoptilolite-Cs	44-1398	$\text{Cs}_{5.5}\text{K}_{0.4}(\text{Al}_7\text{Si}_{29})\text{O}_{72}\cdot 13\text{H}_2\text{O}$
Quartz	05-0490	SiO_2
Quartz	65-0466	SiO_2
Albite	19-1184	$\text{NaAlSi}_3\text{O}_8$
Albite	10-0393	$\text{Na}(\text{Si}_3\text{Al})\text{O}_8$
Helaudite	13-0196	$\text{CaAl}_2\text{Si}_7\text{O}_{18}\cdot 6\text{H}_2\text{O}$
Helaudite	75-1712	$(\text{Na}\cdot 26\text{K}_{0.89}\text{Ca}_{3.37}\text{Sr}_{0.24}\text{Ba}_{0.03})\text{Al}_{9.48}\text{Si}_{26.61}\text{O}_{72}(\text{H}_2\text{O})_{24.84}\text{H}_{1.03}$

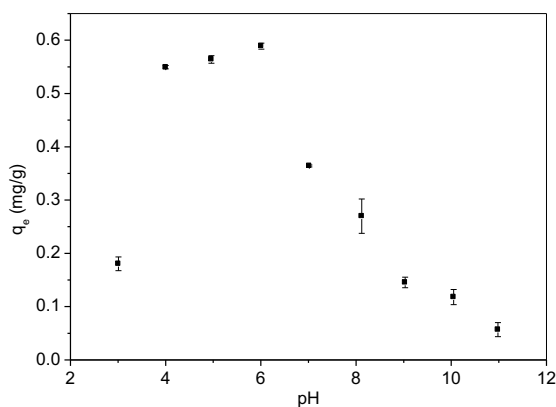


Figure 7 Effect of pH on removal of fluoride ions from solution.

3.2 Effect of pH

The effect of pH on the adsorption capacity of the zeolitic material for fluoride ions presented in Figure 7, the highest removal was at pH values between 4 and 6, according to the point of zero charge, below pH 7.06 the surface charge is positive, which favors the removal of fluoride ions and above that the surface charge is negative, which makes removal less probable (Nabbou *et al.* 2019). In addition, at high or low pH values it is possible that the material may suffer structural alterations that would affect its adsorption capacity, at high pH the hydroxyl ions (OH⁻) probably compete with the fluoride ions for the adsorption sites, and therefore a decrease in the adsorption capacity of the material occurs (Saucedo-Delgado *et al.* 2017).

3.3 Isotherms at different temperatures

Figure 8 shows the isotherms at 20, 30, 40 and 50°C, the isotherms do not show a plateau characteristic of the Langmuir model (Telkapalliwar and Shivankar, 2019), but rather a shape described by the Freundlich model. The lowest removal of fluoride ions was at 20°C and the removal was similar from 30 to 50°C, therefore the thermodynamic parameters could not be calculated in this temperature range.

Table 3 shows the parameters obtained from the fitting of the experimental data to the models of Langmuir and Freundlich, the correlation coefficients are similar for both models, however, the shape of the isotherms suggests a Freundlich type isotherms.

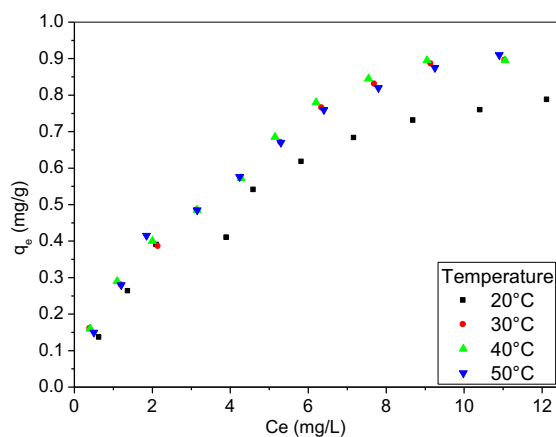


Figure 8 Adsorption isotherms of fluoride ions by the modified zeolitic material at different temperatures.

The results suggest that the adsorption process is carried out through the formation of multilayers on a heterogeneous surface of the adsorbent material (Zhang and Jia, 2018; Zhang *et al.* 2021).

3.4 Adsorption kinetics

Figure 9 shows the relationship between the contact time and the adsorption capacity of the modified zeolitic material, the adsorption is fast at the beginning of the adsorption process and then the equilibrium was reached in 9 hours, the experimental adsorption equilibrium capacity (q_{e_exp}) was 0.57 mg/g.

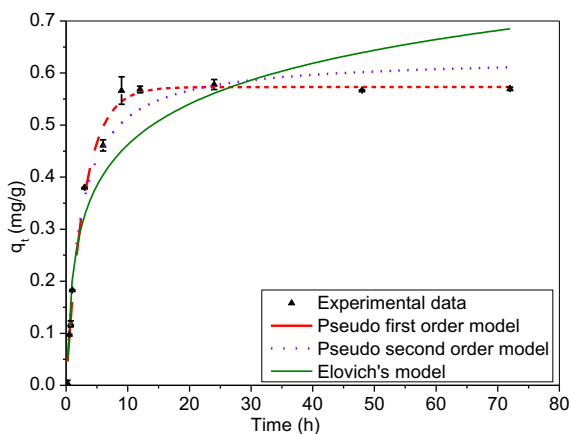


Figure 9. Adsorption kinetics fitted to the models of pseudo first order, pseudo second order and Elovich.

Table 3. Parameters of the isotherms at different temperatures from the experimental data.

T (°C)	Langmuir			Freundlich			
	q_e (mg/g)	q_m (mg/g)	b (L/mg)	R^2	K_F	n	R^2
20	0.78	1.10	0.21	0.97	0.24	1.99	0.96
30	0.86	1.35	0.19	0.98	0.27	1.89	0.98
40	0.86	1.31	0.22	0.97	0.28	1.96	0.97
50	0.91	1.29	0.21	0.99	0.27	1.92	0.99

Table 4 Kinetic parameters for the adsorption of fluoride ions by the modified zeolitic material.

Kinetic model	Parameters	
Pseudo first order	q_{e_exp} (mg/g)	0.56
	q_{e_calc} (mg/g)	0.57
	K_1 (min^{-1})	0.34
	R^2	0.99
Pseudo second order	q_{e_exp} (mg/g)	0.57
	q_{e_calc} (mg/g)	0.63
	K_2 (g/mg-h)	0.11
	R^2	0.97
Elovich	α (mg/g-h)	53.38
	β (mg/g)	0.11
	R^2	0.88

The kinetic parameters were calculated by fitting the experimental data to the pseudo first-order model, the pseudo second-order model, and the Elovich model by using the Origin Lab software and Eq. 1, 2, and 3. The experimental data fit best to the pseudo-first order model.

Table 4 shows the parameters calculated from the experimental data and the models, the results show that the experimental adsorption capacity is similar to the calculated one and the correlation coefficient is the highest for the pseudo first order model, indicating that the mechanism that takes place is physisorption (Flores-Alamo *et al.* 2015). The Elovich model indicates that the adsorption process predominates on the desorption process ($\alpha > \beta$).

3.5 Removal of fluoride ions from drinking water

The modified zeolitic material was tested with drinking water from the state of Zacatecas, Mexico, the pH of the sample was 7.88 and its concentration was 5.46 mg/L, the pH of the sample was adjusted to 6 because the highest adsorption was found at this pH. Figure 10 shows adsorption capacity vs. the dose, the adsorption capacity increases as the dose increases, this is due to the fact that there are more active sites for the adsorption of fluoride ions, a plateau was observed and the maximum adsorption (86.2 %) was found with 90 mg of modified zeolitic material, later there is no longer a considerable difference in the adsorption capacities (Onyango *et al.* 2010).

Conclusions

A zeolitic material was modified with a surfactant and characterized, the Si/Al ratio of 5.11 was determined by scanning electron microscopy (EDS), this value has been commonly reported for heulandite-type zeolites. The increase of carbon in the material after

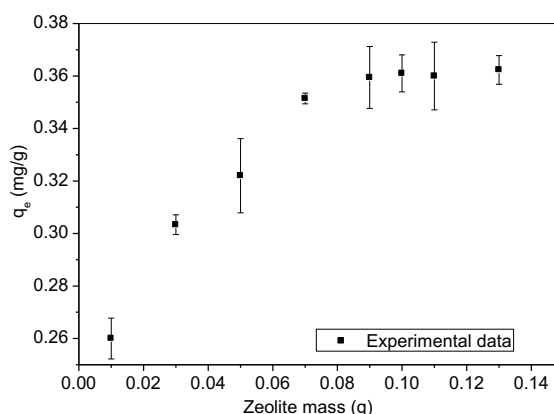


Figure 10. Adsorption capacity vs. dose of adsorbent.

modification indicated the presence of the surfactant in the zeolitic material. The point of zero charge was 7.06, then the maximum removal of fluoride ions was expected at pH lower than this value where the zeolitic material surface is positive.

The kinetic data were best adjusted to the pseudo first-order kinetic model, suggesting that the removal of fluoride ions is carried out by physisorption. The adjustment of the experimental data to the Freundlich model indicates that the adsorption process was carried out through the formation of multilayers on the surface of the modified zeolitic material.

The optimum pH for the removal of fluoride ions is between 4 and 6, with a maximum removal of 57.8 %. The removal of fluoride ions is very similar at different temperatures and the data fit best to the Freundlich model with correlation coefficients of 0.96, 0.98, 0.97 and 0.99 for 20, 30, 40, and 50°C respectively. The highest removal percentage of fluoride ions from drinking water was 86.2% with 90 mg of zeolite. The modified material offers an alternative for removing fluoride ions from water.

Acknowledgements

Authors thank Tecnológico Nacional de México/Instituto Tecnológico de Toluca for financial

support and Consejo Nacional de Humanidades, Ciencias y Tecnologías (CONAHCYT) for the scholarship for master's studies of J.I. Vázquez Méndez.

References

- Ahamad, K., Singh, R., Baruah, I., Choudhury, H. and Sharma, M. (2018). Equilibrium and kinetics modeling of fluoride adsorption onto activated alumina, alum and brick powder. *Groundwater for Sustainable Development*, 7, 452–458. <https://doi.org/10.1016/J.GSD.2018.06.005>
- Alarcón-Herrera, M, Martín-Alarcon, D., Gutiérrez, M., Reynoso-Cuevas, L., Martín-Domínguez, A., Olmos-Márquez, M. and Bundschuh, J. (2020). Co-occurrence, possible origin, and health-risk assessment of arsenic and fluoride in drinking water sources in Mexico: Geographical data visualization. *Science of The Total Environment*, 698, 134168. <https://doi.org/10.1016/J.SCITOTENV.2019.134168>
- Alhassan, S., He, Y., Huang, L., Wu, B., Yan, L., Deng, H. and Wang, H. (2020). A review on fluoride adsorption using modified bauxite: Surface modification and sorption mechanisms perspectives. *Journal of Environmental Chemical Engineering*, 8(6), 104532. <https://doi.org/10.1016/J.JECE.2020.104532>
- Bajda, T. and Kłapyta, Z. (2013). Adsorption of chromate from aqueous solutions by HDTMA-modified clinoptilolite, glauconite and montmorillonite. *Applied Clay Science*, 86, 169-173.
- Barczyk, K., Mozgawa, W. and Król, M. (2014). Studies of anions sorption on natural zeolites. *Spectrochimica Acta Part A: Molecular and Biomolecular Spectroscopy*, 133, 876–882. <https://doi.org/10.1016/J.SAA.2014.06.065>
- Bhatnagar, A., Kumar, E. and Sillanpää, M. (2011). Fluoride removal from water by adsorption—A review. *Chemical Engineering Journal*, 171(3), 811–840. <https://doi.org/10.1016/J.CEJ.2011.05.028>
- Chai, J., Zhang, W., Liu, D., Li, S., Chen, X., Yang, Y. and Zhang, D. (2022). Decreased levels and ecological risks of disinfection by-product chloroform in a field-scale artificial groundwater recharge project by colloid supplement. *Environment International*, 161, 107130. <https://doi.org/10.1016/J.ENVINT.2022.107130>
- Chen, C., Shih, Y., Su, J., Chen, K. and Huang, C. (2022). Mesoporous zirconium pyrophosphate for the adsorption of fluoride from dilute aqueous solutions. *Chemical Engineering Journal*, 427, 132034. <https://doi.org/10.1016/J.CEJ.2021.132034>
- Corral-Capulin, N., Vilchis-Nestor, A., Gutiérrez-Segura, E. and Solache-Ríos, M. (2018). The influence of chemical and thermal treatments on the fluoride removal from water by three mineral structures and their characterization. *Journal of Fluorine Chemistry*, 213, 42–50. <https://doi.org/10.1016/J.JFLUCHEM.2018.07.002>
- Dávila-Estrada, M., Ramírez-García, J. J., Díaz-Nava, M. C., and Solache-Ríos, M. (2016). Sorption of 17 α -ethinylestradiol by surfactant-modified zeolite-rich tuff from aqueous solutions. *Water, Air, & Soil Pollution*, 227, 1-10. <https://doi.org/10.1007/s11270-016-2850-y>
- Dimas Rivera, G., Martínez Hernández, A., Pérez Cabello, A., Rivas Barragán, E., Liñán Montes, A., Flores Escamilla, G., Sandoval Rangel, L., Suarez Vazquez, S. and de Haro Del Río, D. (2021). Removal of chromate anions and immobilization using surfactant-modified zeolites. *Journal of Water Process Engineering*, 39, 101717. <https://doi.org/10.1016/J.JWPE.2020.101717>
- Flores-Alamo, N., Solache-Ríos, M. J., Gómez-Espinosa, R.M. and García-Gaitán, B. (2015). Estudio de adsorción competitiva de cobre y zinc en solución acuosa utilizando Q/PVA/EGDE. *Revista Mexicana de Ingeniería Química*, 14(3), 801-811. <http://www.rmiq.org/ojs311/index.php/rmiq/article/view/995>
- He, J., Yang, Y., Wu, Z., Xie, C., Zhang, K., Kong, L. and Liu, J. (2020). Review of fluoride removal from water environment by adsorption. *Journal of Environmental Chemical Engineering*, 8(6), 104516. <https://doi.org/10.1016/J.JECE.2020.104516>
- Hosseinfard, S., Aroon, M. and Dahrazma, B. (2020). Application of PVDF/HDTMA-modified clinoptilolite nanocomposite membranes in removal of reactive dye from aqueous solution. *Separation and Purification Technology*, 251, 117294. <https://doi.org/10.1016/J.SEPPUR.2020.117294>

- Jiang, P., Li, G., Zhou, X., Wang, C., Qiao, Y., Liao, D. and Shi, D. (2019). Chronic fluoride exposure induces neuronal apoptosis and impairs neurogenesis and synaptic plasticity: Role of GSK-3 β / β -catenin pathway. *Chemosphere*, 214, 430–435. <https://doi.org/10.1016/J.CHEMOSPHERE.2018.09.095>
- Kabuba, J. and Banza, M. (2020). Ion-exchange process for the removal of Ni (II) and Co (II) from wastewater using modified clinoptilolite: Modeling by response surface methodology and artificial neural network. *Results in Engineering*, 8, 100189. <https://doi.org/10.1016/J.RINENG.2020.100189>
- Liu M., Zang, Z., Zhang, S., Ouyang, G. and Han, R. (2021). Enhanced fluoride adsorption from aqueous solution by zirconium (IV)-impregnated magnetic chitosan graphene oxide. *International Journal of Biological Macromolecules*, 182, 1759–1768. <https://doi.org/10.1016/J.IJBIOMAC.2021.05.116>
- Leal-Perez, J. E., Almaral-Sanchez, J. L., Hurtado-Macias, A., Cortez-Valadez, M., Bórquez-Mendivil, A., García-Grajeda, B. A. and Flores-Valenzuela, J. (2024). Structural and chemical analysis of Zn ion exchange in thermally modified zeolite A4. *Revista Mexicana de Ingeniería Química*, 23(3). <https://doi.org/10.24275/rmiq/Mat24264>
- López-Guzmán, M., Alarcón-Herrera, M., Irigoyen-Campuzano, J., Torres-Castañón, L. and Reynoso-Cuevas, L. (2019). Simultaneous removal of fluoride and arsenic from well water by electrocoagulation. *Science of The Total Environment*, 678, 181–187. <https://doi.org/10.1016/J.SCITOTENV.2019.04.400>
- Martínez-Salazar, E., Flores-Rodríguez, V., Rosas-Valdez, R. and Falcón-Ordaz, J. (2016). Helminth parasites of some rodents (Cricetidae, Heteromyidae, and Sciuridae) from Zacatecas, Mexico. *Revista Mexicana de Biodiversidad*, 87(4), 1203–1211. <https://doi.org/10.1016/J.RMB.2016.10.009>
- Mohapatra, M., Anand, S., Mishra, B., Giles, D. and Singh, P. (2009). Review of fluoride removal from drinking water. *Journal of Environmental Management*, 91(1), 67–77. <https://doi.org/10.1016/J.JENVMAN.2009.08.015>
- Nabbou, N., Belhachemi, M., Boumelik, M., Merzougui, T., Lahcene, D., Harek, Y., Zorpas, A. and Jeguirim, M. (2019). Removal of fluoride from groundwater using natural clay (kaolinite): Optimization of adsorption conditions. *Comptes Rendus Chimie*, 22(2–3), 105–112. <https://doi.org/10.1016/J.CRCI.2018.09.010>
- Naghash, A. and Nezamzadeh-Ejehieh, A. (2015). Comparison of the efficiency of modified clinoptilolite with HDTMA and HDP surfactants for the removal of phosphate in aqueous solutions. *Journal of Industrial and Engineering Chemistry*, 31, 185–191. <https://doi.org/10.1016/J.JIEC.2015.06.022>
- Navarro, O., González, J., Júnez-Ferreira, H., Bautista, C. and Cardona, A. (2017). Correlation of Arsenic and Fluoride in the Groundwater for Human Consumption in a Semiarid Region of Mexico. *Procedia Engineering*, 186, 333–340. <https://doi.org/10.1016/J.PROENG.2017.03.259>
- Nezamzadeh-Ejehieh, A. and Tavakoli-Ghinani, S. (2014). Effect of a nano-sized natural clinoptilolite modified by the hexadecyltrimethyl ammonium surfactant on cephalixin drug delivery. *Comptes Rendus Chimie*, 17(1), 49–61. <https://doi.org/10.1016/J.CRCI.2013.07.009>
- Nizam, S., Virk, H. S. and Sen, I. (2022). High levels of fluoride in groundwater from Northern parts of Indo-Gangetic plains reveals detrimental fluorosis health risks. *Environmental Advances*, 8, 100200. <https://doi.org/10.1016/J.ENVADV.2022.100200>
- Jiménez-Reyes, M., Almazán-Sánchez, P., and Solache-Ríos M. (2021). Radioactive waste treatments by using zeolites. A short review. *Journal of Environmental Radioactivity*. 233, 106610. <https://doi.org/10.1016/j.jenvrad.2021.106610>
- Onyango, M., Masukume, M., Ochieng, A. and Otieno, F. (2010). Functionalised natural zeolite and its potential for treating drinking water containing excess amount of nitrate. *Water Research Commission*, 36, 655–662. <https://doi.org/10.4314/wsa.v36i5.61999>
- Saadat, M., and Nezamzadeh-Ejehieh, A. (2016). Clinoptilolite nanoparticles containing HDTMA and Arsenazo III as a sensitive carbon paste electrode modifier for indirect voltammetric measurement of Cesium ions. *Electrochimica Acta*, 217, 163–170. <https://doi.org/10.1016/J.ELECTACTA.2016.09.084>

- Saucedo-Delgado, B., Haro, D., González-Rodríguez, L., Reynel-Ávila, H., Mendoza-Castillo, D., Bonilla-Petriciolet, A. and Rivera de la Rosa, J. (2017). Fluoride adsorption from aqueous solution using a protonated clinoptilolite and its modeling with artificial neural network-based model. *Journal of Fluorine Chemistry*, 204, 98–106. <https://doi.org/10.1016/J.JFLUCHEM.2017.11.002>
- Serrano-Meza, A., Viguera-Cortes, J. M., and Allen, C. D. (2024). Municipal wastewater treatment in a hybrid biofiltration system packed with agave fiber. *Revista Mexicana de Ingeniería Química*, 23(3). <https://doi.org/10.24275/rmiq/Mat24264>
- Solińska, A. and Bajda, T. (2022). Modified zeolite as a sorbent for removal of contaminants from wet flue gas desulphurization wastewater. *Chemosphere*, 286. <https://doi.org/10.1016/J.CHEMOSPHERE.2021.131772>
- Telkapalliwar, N. and Shivankar, V. (2019). Data of characterization and adsorption of fluoride from aqueous solution by using modified *Azadirachta indica* bark. *Data in Brief*, 26. <https://doi.org/10.1016/J.DIB.2019.104509>
- Ullah, R., Liu, C., Panezai, H., Gul, A., Sun, J. and Wu, X. (2020). Controlled crystal phase and particle size of loaded-TiO₂ using clinoptilolite as support via hydrothermal method for degradation of crystal violet dye in aqueous solution. *Arabian Journal of Chemistry*, 13(2), 4092–4101. <https://doi.org/10.1016/J.ARABJC.2019.06.011>
- Wingenfelder, U., Furrer, G. and Schulin, R. (2006). Sorption of antimonate by HDTMA-modified zeolite. *Microporous and Mesoporous Materials*, 95, 265–271. <https://doi.org/10.1016/J.MICROMESO.2006.06.001>
- Zeng, Y., Woo, H., Lee, G. and Park, J. (2010). Removal of chromate from water using surfactant modified Pohang clinoptilolite and Haruna chabazite. *Desalination*, 257, 102–109. <https://doi.org/10.1016/J.DESAL.2010.02.039>
- Zhang, X., Qi, Y., Chen, Z., Song, N., Li, X., Ren, D., & Zhang, S. (2021). Evaluation of fluoride and cadmium adsorption modification of corn stalk by aluminum trichloride. *Applied Surface Science*, 543, 148727. <https://doi.org/10.1016/j.apsusc.2020.148727>
- Zhang, Y. and Jia, Y. (2018). Fluoride adsorption on manganese carbonate: Ion-exchange based on the surface carbonate-like groups and hydroxyl groups. *Journal of Colloid and Interface Science*, 510, 407–417. <https://doi.org/10.1016/J.JCIS.2017.09.090>
- Znak, Z., Zin, O., Mashtaler, A., Korniy, S., Sukhatskiy, Y., Gogate, P. R., Mnykh, R. and Thanekar, P. (2021). Improved modification of clinoptilolite with silver using ultrasonic radiation. *Ultrasonics Sonochemistry*, 73, 105496. <https://doi.org/10.1016/J.ULTSONCH.2021.105496>